J. SOULARD, B. MULTON, J. LUCIDARME, M. LÉCRIVAIN, L. PRÉVOND, « Modelling, Analysis of Parameters and Tests of a Small Electronically Commutated Single-Phase Permanent-Magnet Reluctance Motor. », ICEM'96, Vigo, 10-12 sept. 96, Vol.2, pp.45-50.

Modelling, Analysis of Parameters and Tests of a Small Electronically Commutated Single-Phase Permanent Magnet Reluctance Motor

J. SOULARD, B. MULTON, J. LUCIDARME, M. LECRIVAIN, L. PREVOND

LESIR URA CNRS D1375 E-Mail: Juliette.Soulard@lesir.ens-cachan.fr
Ecole **N**ormale **S**upérieure de **C**achan
61, avenue du Président Wilson 94235 Cachan Cédex FRANCE

Abstract

The aim of this study is to evaluate the field flux in a small electronically commutated single-phase permanent magnet reluctance motor. Its structure is inherently three-dimensional. An analytical model is built so that an analysis of parameters can be easily conducted.

With a first simple model, an optimum is found for the magnets' length that may permit to use disk-magnet technology. Yet, the value of the field flux lacks accuracy. In order to locate the main leakage fluxes, the finite element analysis is used on a bidimensional equivalent geometry. A second and satisfying analytical model is determined.

Experimental results confirm the effectiveness of the model to fulfil analysis of parameters.

Keywords

Small permanent magnet reluctance motor
Single phase motor
Analytical magnetic model
Finite element analysis

Introduction

This study deals with a single-phase permanent magnet motor from the class of the flux-switching machines [1]. This innovating structure allowing the starting without stator or rotor disymmetry [2] is easy to miniaturise. The single solenoid-shaped winding can have small dimensions with a good filling-factor, while the magnets in the stator allow good performances with high flux concentration [3,4,5]. Its massive rotor, without any windings nor permanent magnets, can be easily miniaturised too.

The purpose of this paper is to build an analytical model of the three-dimensional electromagnetic structure.

After a description of the motor and of its principle, a first model is built up and an optimal magnet length is found. Finite element analysis is used to improve the model. A 2D finite element software requires the elaboration of an equivalent two-dimensional geometry. Then, a prototype is designed with a second improved analytical model.

To conclude on the model's validity and its future use, measurements are carried out on the prototype with several rotors.

Description and principle of the motor

Figure 1 shows the four-pole machine with its four NdFeB permanent magnets (PM).

The electromagnetic parts are made of steel and the frame of aluminium. The motor has a 11 mm external diameter. It is 11.5 mm long.

The winding is a simple solenoid coil, around the axial piece of the rotor. The design principle, so that the motor can start, is described later in this paper.

The active air gap e_1 has minimum and maximum reluctance values, though e_2 is a constant air gap.

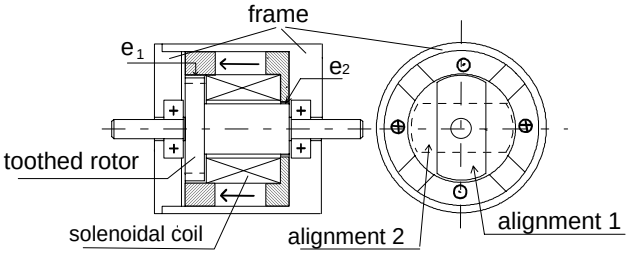

Figure 1 : Cross-sections of the motor

The flux linkage ψ is alternative and its amplitude is high. One pair of magnets mainly produces it in alignment 1. In alignment 2, it is the other pair with an other sign. When the rotor turns, a back EMF is induced in the winding. A square-wave winding current with an amplitude of I_M creates an hybrid torque.

The average torque value is maximum if there is no phase shift between the current and the back EMF. Figure 2 a-b show the current, EMF and flux linkage wave forms (the flux linkage is assumed to be a sinusoidal function of the position) and the magnetic cycle ψ(nI) associated to this ideal case.

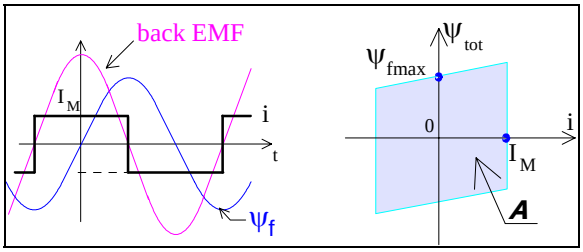

Figure 2 : a- Wave forms (constant speed)
b- Energy conversion stroke

The area **A** of the cycle represents the converted energy so the average torque value T is :

$$T = \frac{\mathbf{A}.p}{2.\pi}.$$

In this particular case (square-wave current), $\mathbf{A} = 4.\psi_{f\,max}.I_M$, so

$$T = \left(\frac{2p}{\pi}\right).\psi_{f\,max}.I_M = \left(\frac{2p}{\pi}\right).\varphi_{f\,max}.(nI_M) \qquad (1)$$

with $\psi_{f\,max}$ amplitude of field flux linkage
2p number of poles (p=2)
n number of turns
$\varphi_{f\,max} = \frac{\psi_{f\,max}}{n}$ amplitude of the field flux

The value of the current is limited by thermal considerations. In this small motors, the copper losses are dominating so the equation is :

$$Pj = \frac{\Delta T}{Rth} = \pi.\rho.\delta^2.\mathbf{l}_w.k_b.\left(r_{we}{}^2 - r_{wi}{}^2\right) \qquad (2)$$

with ΔT : allowed temperature raising
R_{th} : thermal resistance coil-ambient
ρ : copper resistivity at T=80°C
δ : current density
k_b : filling factor (≈ 0.5)
$\mathbf{l}_w$: coil length
r_{we} and r_{wi} : coil external and internal radius
(see annexe for the motor's sizes)

The current density depends on the winding dimensions and the current rms value :

$$\delta = \frac{nI_{rms}}{k_b.\mathbf{l}_w.(r_{we} - r_{wi})} \qquad (3)$$

In this study, the current is supposed to be a square wave so $nI_{eff} = nI_{max}$.

With (1), (2) and (3), the maximum value for the current is given by :

$$(nI)_{max} = \sqrt{\frac{\Delta T}{R_{th}}.k_b.\frac{1}{\pi}.\mathbf{l}_w.\frac{1}{\rho}.\frac{r_{we} - r_{wi}}{r_{we} + r_{wi}}} \qquad (4)$$

If external sizes and the number of poles are set, the only way to improve the mean torque is to determine the electromagnetic geometry that maximise the field flux φ_{fmax}.

Therefore, the aim of this study is to evaluate the amplitude of the field flux φ_{fmax} , that is the maximum value of the flux created by the PM inductor in the rotor section. It depends on the motor's geometry and the PM magnetic characteristics.

First-level analytical model

The magnetic circuit is assumed to be non-saturated. The rotor is in one of the aligned positions (maximum of the field flux).

The first model, shown in figure 3, considers only the main path for each PM flux without taking into account the leakage flux.

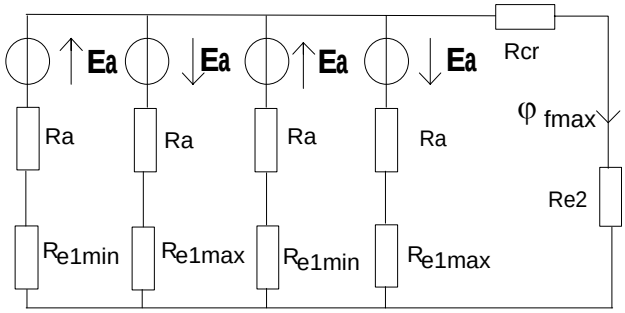

Figure 3 : First-level analytical model

$\mathbf{E}_a = \frac{B_r.\ell_a}{\mu_0.\mu_a}$ magneto motive force (MMF) of one magnet

$R_a = \frac{\ell_a}{\mu_0.\mu_a.S_a}$ magnet reluctance

(with $\mathbf{l}_a$ magnet length and S_a magnet cross section)

R_{e1max}, R_{e1min} maximum and minimum active air gap reluctance

R_{cr} rotor reluctance

R_{e2} constant air gap reluctance

The maximum value of the field flux is given by equation (5). It is related to the different reluctance, the magnet cross section S_a, and the magnet residual flux density B_r.

$$\varphi_{f\,max} = \frac{2.B_r.R_a.(R_{e1max} - R_{e1min}).S_a}{R_a^2 + \alpha.R_a + \beta} \qquad (5)$$

with

$$\alpha = \left(R_{e1max} + R_{e1min} + 4.(R_{cr} + R_{e2})\right)$$

$$\beta = 2.(R_{e1max} + R_{e1min}).(R_{cr} + R_{e2}) + R_{e1max}.R_{e1min}$$

The function $\frac{\varphi_{f\,max}}{S_a}(R_a)$ admits a maximum for

$$R_{aopt} = \sqrt{\beta}. \qquad (6)$$

Notice that if $R_{cr} = R_{e2} = 0$ then $\beta = R_{e1max}.R_{e1min}$.

If the magnet cross section is set by the radial dimensions of the structure, there is an optimal magnet length. It is given by :

$$\ell_{aopt} = \mu_0 . \mu_a . S_a . \sqrt{\beta} \qquad (7)$$

Measurements made on a prototype show differences to the model's values that reach 50 %. Indeed, the leakage flux were not taken into account. Therefore, an improved model was developed.

Second-level analytical model based on finite element analysis

With finite element analysis, the main leakage flux paths can be located and then corresponding reluctance were added to the analytical model. The motor has a three-dimensional electromagnetic structure. Therefore, an equivalent two-dimensional geometry (figure 4) was established in order to use a 2D software (Maxwell2D Ansoft Corp.)

Equivalent geometry

It is calculated so that ratios of reluctance are the same as in the motor. The symmetry of the structure allows to study only half of the motor.

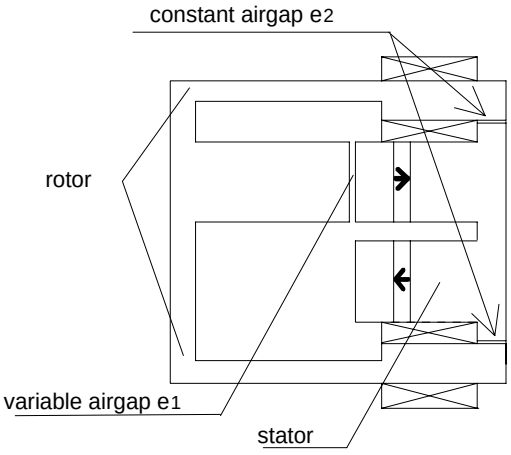

Figure 4 : Two-dimensional equivalent structure

The permanent magnet is developed along its mean area (figure 5). As the magnet's reluctance is the reference, the third dimension of the equivalent geometry is the PM thickness : e_a=2.05 mm.

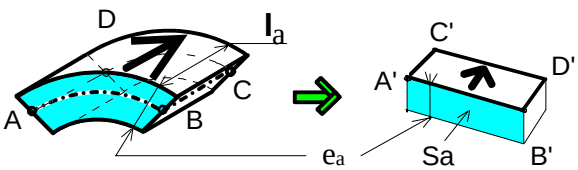

Figure 5 : PM and equivalent PM

In part n°1, the path of the flux is as shown in figure 6. The length-section ratio is 0.23 so the equivalent length is $l_2 = 0.23 * S_a$.

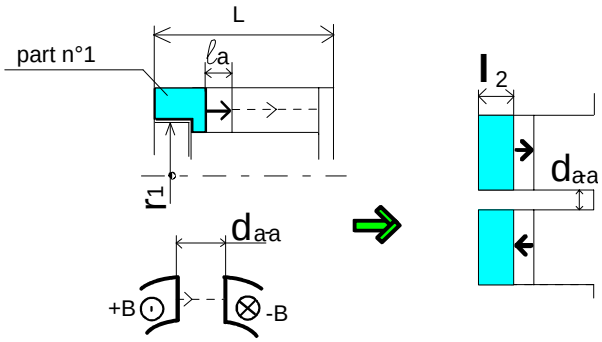

Figure 6 : Part n°1 and interpolar area equivalents

Half of the motor is modelled but there can be a leakage flux with both the adjacent poles. Therefore, the equivalent interpolar distance $d_{a\text{-}a\ eq}$ is half of the real one (figure 6).

The difficult point is to define the equivalent rotor as it becomes a two-part piece with a geometry very different from the real one.

Second analytical model

Flux lines in figure 7 show that the main flux leakage are located in the interpolar area.

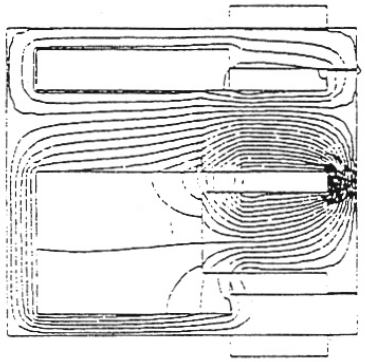

Figure 7 : Flux lines for the equivalent geometry

Four leakage reluctances were therefore added to the first-level analytical model (figure 8).

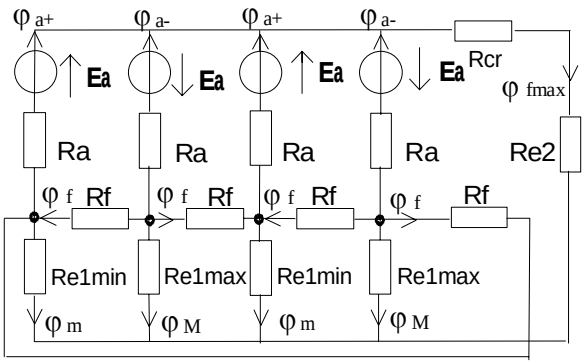

Figure 8 : Second-level analytical model

The complexity of the model now requires a description with matrix equations. The variation of $\varphi_{f\,max}$ as a function of the magnet length is shown in figure 9.

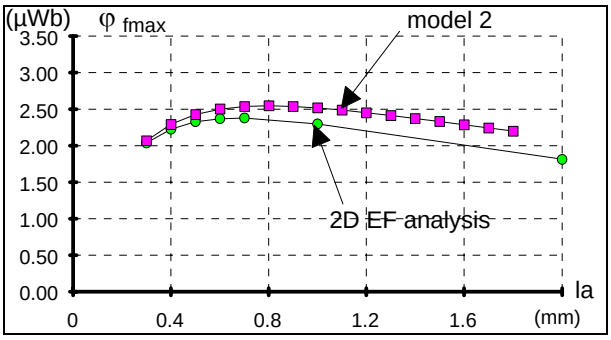

Figure 9 : φ_{fmax} versus the magnet length (rotor arc pole $\beta r = 60°$)

With both methods, the optimal length is 0.7 mm, leading to very thin magnets. The maximum of the difference between the two graphs is less than 10 %, so the improved model was used to optimise the magnet length of a second prototype.

Starting solution

In motors with permanent magnets, there are several types of position with a null detent torque (T_{detent}) : the stable and the unstable ones.

In the studied structure, the aligned position (figure 10-a) is a natural stable stopping point (detent position). Thus, the rotor is likely to stop in this position. Unluckily, the hybrid torque is null there so the motor can not start.

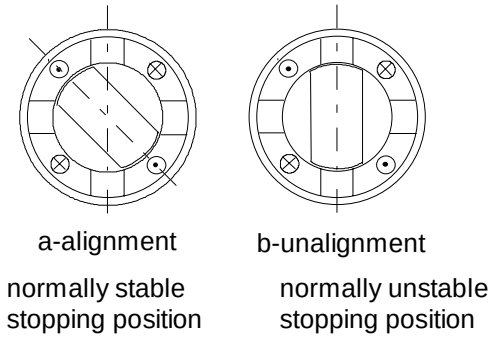

Figure 10 : Positions where $T_{detent} = 0$

The hybrid torque in the unaligned position is maximal so there is no problem to start. Yet, as it is an naturally unstable stopping point, the rotor is less likely to stop there.

One solution [2] is to modify the electromagnetic geometry so that the unaligned positions are also stopping stable points. This is possible with enlarging the rotor arc pole. Figure 11 shows the geometry of the enlarged rotor.

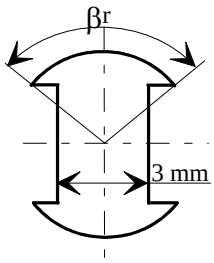

Figure 11 : Geometry of the enlarged rotor

If the rotor arc pole is larger, the air gap reluctance in unaligned positions is smaller so the magnet flux are higher. So there is a value that permits the total magnet flux to be higher in the unaligned positions then in the aligned ones. Unaligned positions have become stable stopping points and the aligned ones unstable. Thus, the rotor stops in positions where it can start.

The drawback of this solution is the maximum of the field flux is reduced when the rotor is larger (figure 13) so the average torque is smaller.

Experimental results

The second analytical model was used to calculate the dimensions of the magnetic circuit of a new prototype, according to thermal and mechanical constraints.

Maximum of the field flux

The obtained optimal magnet length is 0.6 mm. The magnets in the motor are 1 mm long because of our machining possibilities. This reduces the theoretic value of φ_{fmax} of 5 % (figure 12).

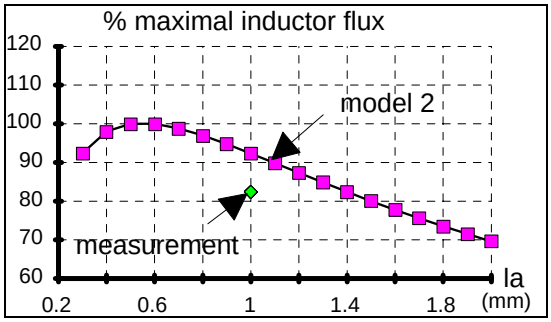

Figure 12 : φ_{fmax} sensibility versus magnet length with second analytical model ($e_1 = 0.015mm$, $e_2 = 0.025mm$, $\beta r = 100°$)

Measurements were performed with rotors of several arc poles (starting considerations [2,6]). Differences shown in figure 13 between measurements and model's values are in the expected range from 10 to 15%. A more complicated model (model 3), also taking into account winding flux leakage, gives better results (less than 8 %).

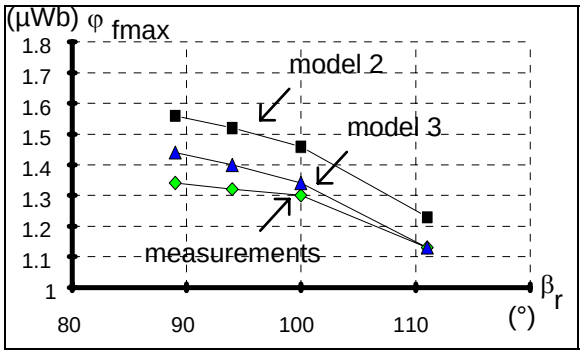

Figure 13 : Measured and computed flux versus rotor arc pole β_r
($\ell_a = 1\text{mm}$, $e_1 = 0.015\text{mm}$, $e_2 = 0.025\text{mm}$)

Field flux and theoretical average torque value

The following measurements were performed with the same rotor. The main dimensions are : $\ell_a = 1\text{mm}$, $e_1 = 0.015\text{mm}$, $e_2 = 0.065\text{mm}$, $\beta_a = 80.5°$.

Figure 14 shows the forms of the no-load tension and the numerically integrated flux for a speed of 3676 rpm. The flux wave-form is quite sinusoidal.

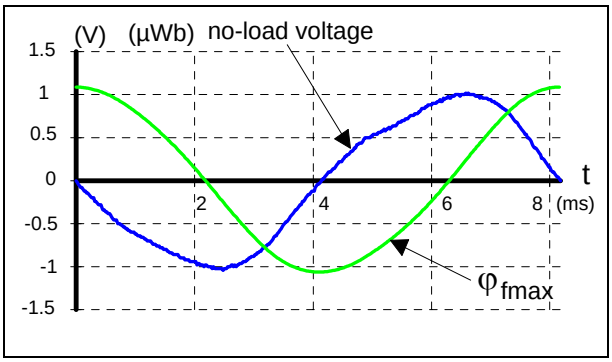

Figure 14 : No-load voltage and numerically integrated field flux at 3676 rpm
($\ell_a = 1\text{mm}$, $e_1 = 0.015\text{mm}$, $e_2 = 0.065\text{mm}$, $\beta_a = 80.5°$)

In the prototype, the sizes are : $r_{we} = 3\text{mm}$, $r_{wi} = 1.2\text{mm}$ and $l_w = 4.8\text{mm}$. The coil has 1200 turns. The thermal resistance coil-ambient value was estimated to be $R_{th} = 168\text{K / W}$. The allowed temperature raising is ΔT=60K.

Equation (2) gives the maximum of the iron losses : $P_{jmax} = 0.36\text{W}$. The maximum value of $(nI)_{rms}$ is then $(nI)_{max}$=69.2A (4). The correspondent value of a square-wave current is $I_M = 57.7\text{mA}$.

With the measured value of the field flux $\varphi_{fmax} = 1.1\mu\text{Wb}$, equation (1) gives the theoretical maximum value of the average torque : T=0.097 mN.m.

Wave-forms and electrical simulation

A square-wave voltage was applied to the prototype. The converter was a full-bridge inverter. It was implemented with an integrated circuit (SN 754410). The switches were Darlington transistors with diodes.

In figure 15, the voltage applied to the motor, the measured current and the simulated one are shown. The speed was constant (with high inertia). The voltage and back EMF had no phase shift.

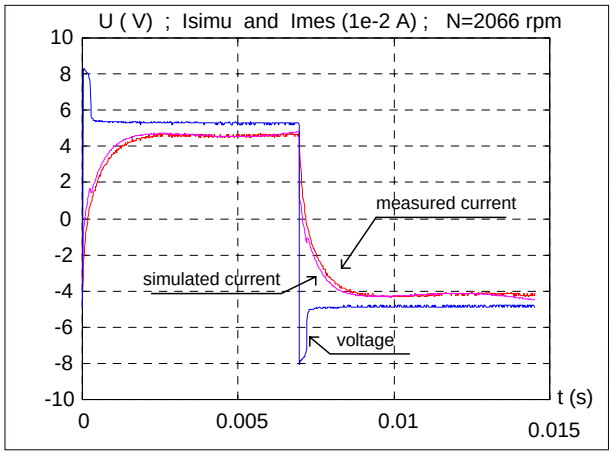

Figure 15 : Voltage and current wave forms (simulation and measurements) at N = 2066 rpm
($\ell_a = 1\text{mm}$, $e_1 = 0.015\text{mm}$, $e_2 = 0.065\text{mm}$, $\beta_a = 80.5°$)

The simulation was made with simulink, toolbox in the software Matlab. The values of R, L and $\psi(\theta)$ were measured to be used in the simulation ($R = 104\Omega$, L = 44mH, and $\psi_{fmax} = 1.3\text{mWb}$).

The mean value of the simulated hybrid torque is 0.068 mN.m. It is 7% lower than the value obtained with (1) because the current wave-form is not a perfect square. The difference here is acceptable because of the uncertainty on φ_{fmax} due to the analytical model.

Yet, the expression of the torque's mean value (1) will not be suitable around the base speed (10 000 rpm) because of the higher rise time of the current.

Therefore, the optimisation of this motor requires a global study of the motor and its inverter, in order to take into account the electrical parameters such as the resistor and the inductance of the winding.

Conclusion

This paper describes a new electromagnetic favourable structure to realise a small electric motor (sizes of several millimetres).

In order to analyse geometrical parameter sensitivity, an analytical model was developed step by step to evaluate the maximum inductor flux. The first-level model led to an expression of an optimal magnet length. Finite element analysis showed important interpolar leakage flux, which were taken into account in the second-level model.

Experiments validated the second-level model. Therefore, it can be used to make a complete parameter analysis of the electromagnetic structure.

The small thickness of the optimised magnets may permit the use of disc-magnet technology. This technology is now well-known and well-controlled in motors with rotating magnets [7].

The next stage will consist of the global optimisation of the motor and its electronic converter (full-bridge inverter). In this study, the inductance and the resistance of the phase, the iron losses will be taken into account.

References

[1] NASAR S, BOLDEA I, UNNEWEHR L ;
"Permanent magnet, reluctance, and self-synchronous motors" ; CRC Press 1993.

[2] LUCIDARME J, MULTON B, PREVOND L ; "Actionneurs hybrides monophasés à commutation de flux" ; french patent CNRS n° F94/12063 (10/10/94).

[3] AMARATUNGA G, ACARNLEY P, MCLAREN P ;
"Optimum magnetic circuit configurations for permanent magnet aerospace generators" ;
IEEE Trans. on Aerospace and Electronic Systems, march 1985, pp 230-255.

[4] LIAO Y, LIPO T ;
"Sizing and optimal design of doubly salient permanent magnet motor" ;
in proceedings of IEE 6th Electric Machines and Drives 1993, pp 452-456.

[5] CRIVII M, JUFER M ;
"A new hybrid switched reluctance motor" ;
in proceedings of ICEM sept. 1994, vol. 2, pp 17-20.

[6] PREVOND L ;
"Study, experiment and modelling of new rotating and linear hybrid structures" ;
Ph.D dissertation, CNAM 1994 (in french).

[7] CLAUDET R, ANTOGNINI A ;
"Un nouveau petit moteur pas-à-pas à aimant disque à double étage" ;
in proceedings of EPE Drives, oct 94, pp 315-320 (English version available at Portescap).

Annexe

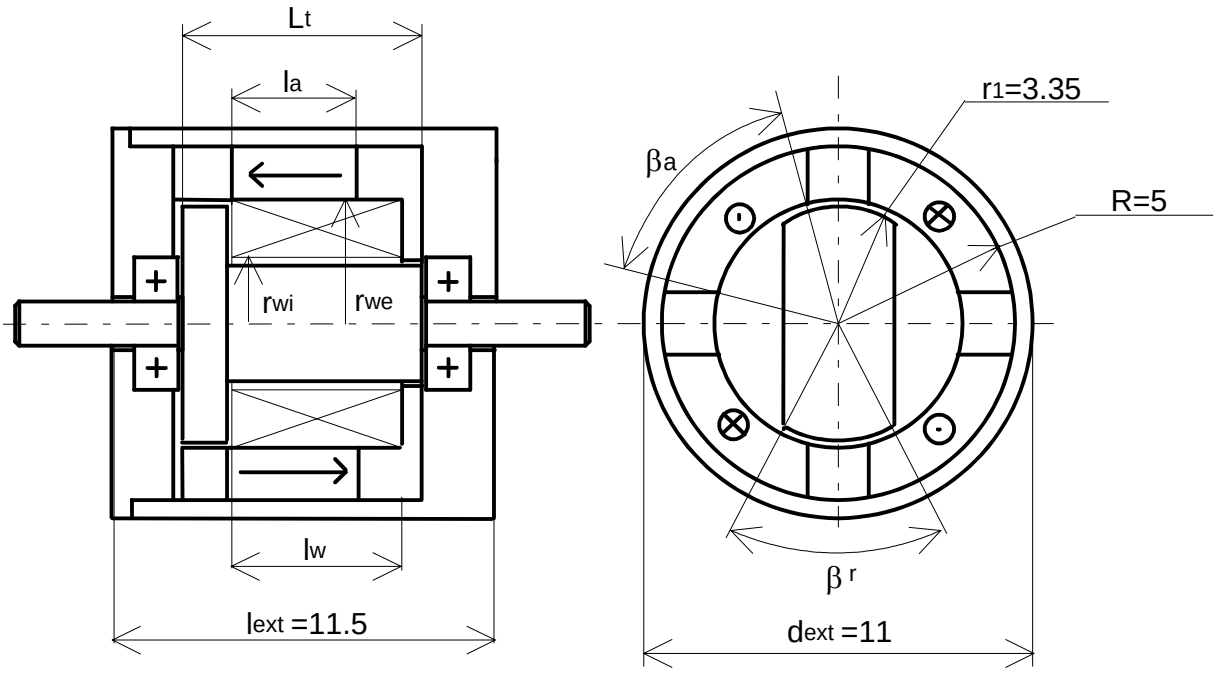

Main dimensions of the prototype

(rotor arc pole β_r and magnet length l_a are adjustable geometric parameters)